

# EXTENSIVE AIR SHOWER SIMULATIONS WITH *CORSIKA* AND THE INFLUENCE OF HIGH-ENERGY HADRONIC INTERACTION MODELS

D. HECK FOR THE **KASCADE** COLLABORATION

*Institut für Kernphysik, Forschungszentrum Karlsruhe, D-76021 Karlsruhe,  
Germany  
E-mail:heck@ik3.fzk.de*

When high-energy cosmic rays ( $\gamma$ 's, protons, or heavy nuclei) impinge onto the Earth's atmosphere, they interact at high altitude with the air nuclei as targets. By repeated interaction of the secondaries an 'extensive air shower' (EAS) is generated with huge particle numbers in the maximum of the shower development. Such cascades are quantitatively simulated by the Monte Carlo computer program *CORSIKA*. The most important uncertainties in simulations arise from modeling of high-energy hadronic interactions: a) The inelastic hadron-air cross sections. b) The energies occurring in EAS may extend far above the energies available in man-made accelerators, and when extrapolating towards higher energies one has to rely on theoretical guidelines. c) In collider experiments which are used to adjust the interaction models the very forward particles are not accessible, but just those particles carry most of the hadronic energy, and in the EAS development they transport a large energy fraction down into the atmosphere.

*CORSIKA* is coupled alternatively with 6 high-energy hadronic interaction codes (DPMJET, HDPM, NEXUS, QGSJET, SIBYLL, VENUS). The influence of those interaction models on observables of simulated EAS is discussed.

## 1 Introduction

*CORSIKA* (**CO**smic **R**ay **SI**mulation for **KA**scade) is a detailed Monte Carlo program to study the evolution of extensive air showers (EAS) in the atmosphere initiated by various cosmic ray particles. Originally, it was designed to perform simulations for the **KASCADE** experiment<sup>1</sup> at Karlsruhe and has been refined considerably since its first version in 1989. Meanwhile, it has developed into a tool that is used for more than 30 experiments worldwide. The prediction of particle energy spectra, densities or arrival times to be observed in EAS experiments is a well suited application of *CORSIKA*. A detailed description of the physics incorporated in *CORSIKA* is given in Ref.<sup>2</sup>, technical details on the handling of the program are described elsewhere.<sup>3</sup>

## 2 EAS Environment Parameters and Particle Transport

To simulate the evolution of EAS global parameters have to be specified: The Earth's magnetic field affecting the movement of charged particles as

well as the atmospheric model to be employed in the simulation depend on the geographic location. CORSIKA provides several atmospheric parameter sets covering the complete climatical and seasonal influence from tropical, subtropical, and mid-latitude regions to the South pole (4 seasons). The composition of air is adopted to 78.1% N<sub>2</sub>, 21.0% O<sub>2</sub> and 0.9% Ar (volume fractions).

Within CORSIKA, various particles are followed: Besides  $\gamma$ -rays the leptons  $e^\pm$  and  $\mu^\pm$  ( $\nu_e$  and  $\nu_\mu$  optionally), the mesons  $\pi^0$ ,  $\pi^\pm$ ,  $K_{S/L}^0$ ,  $K^\pm$  and  $\eta$ , the nucleons, the strange baryons with strangeness  $|S| \leq 3$ , and the corresponding anti-baryons as well as nuclei with  $A \leq 60$  are treated. Mesonic ( $\rho, \omega, K^*$ ) and baryonic ( $\Delta$ ) resonances are decaying without transport.

For each particle its transportation range is estimated. For instable particles both ranges for interaction (determined by cross section) and decay (limited by lifetime) are evaluated independently and the shorter one determines the fate of the particle at the end of its range. In decays, all branches down to the 1 % level are considered with correct kinematics in the 3-body decays. In the range determination of decaying charged particles, the ionization energy loss is considered, which especially affects muons at energies below  $\approx 10$  GeV because of their long lifetime and low interaction cross section. This treatment slightly favors the decay of charged pions - the main source of muons - at the expense of pion-induced interactions, dependent on energy and height of pion origin. During transport, the deflection of charged particles by the Earth's magnetic field is considered.

In CORSIKA, electrons and gammas are treated in a tailored version of the EGS4 code<sup>4</sup> and/or, less detailed but much faster, by analytical NKG-formulas.<sup>5</sup> The electromagnetic interactions are believed to be treated correctly even at the highest energies by taking into account the Landau-Pomeranchuk-Migdal effect. Cherenkov photons may be generated optionally. Hadronic interactions with energies  $E_{\text{lab}} \leq 80$  GeV are modeled by the GHEISHA code<sup>6</sup> or, alternatively, by the UrQMD model.<sup>7</sup>

### 3 Hadronic Interaction Models

The largest uncertainties in numerical simulation of EAS with primary energies above some TeV are induced by the models which describe the hadronic interactions. Especially when extrapolating to the highest energies, where the collision energies exceed those accessible by accelerators, one has to rely on theoretical guidelines to describe the interactions. Additional uncertainties stem from the fact that just those interaction products emitted at small angles into the extreme forward direction carry away the largest energy fraction,

Table 1. Essential features of hadronic interaction models.

Model Version	VENUS 4.12	neXus 2	QGSJET	DPMJET II.4/II.5	SIBYLL 1.6/2.1	HDPM
Gribov-Regge	+	+	+	+		
Mini-Jets		+	+	+	+	
Sec. Interactions	+	+				
N-N interaction	+	+	+	+		
Superposition					+	+
Max. Energy (GeV)	$2 \cdot 10^7$	$2 \cdot 10^8$	$>10^{11}$	$>10^{11}$	$>10^{11}$	$10^8$
Memory (Mbyte)	21	101	10	52	9	8
CPU-Time <sup>1</sup> (min)	4.5	$\approx 100$	1.0	3.5	0.75	1.0

<sup>1</sup> for showers with primary p,  $E_0 = 10^{15}$  eV, vertical,  $E_h, E_\mu \geq 0.3$  GeV, 110 m a.s.l., NKG option, DEC 3000/600 AXP (175 MHz)

but in collider experiments those particles disappear in the beam pipe without being observable. In the development of EAS, such particles are responsible for transporting the energy down into the atmosphere.

To study the influence of models on the uncertainties of EAS observables and on their correlations, 6 different hadronic interaction codes DPMJET<sup>8</sup>, HDPM<sup>2</sup>, NEXUS<sup>9</sup>, QGSJET<sup>10</sup>, SIBYLL<sup>11,12</sup>, and VENUS<sup>13</sup> have been coupled with CORSIKA. They describe the hadronic interactions at energies  $E_{\text{lab}} \geq 80$  GeV. Their basic features are summarized in Table 1.

#### 4 Cross Sections

The longitudinal development of hadronic EAS depends crucially on the inelastic hadron-air cross section. Lower cross sections elongate, higher ones shorten the longitudinal development. Fortunately, the situation has improved

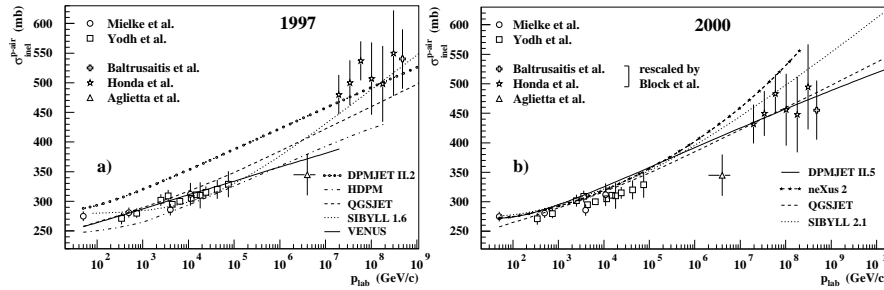


Figure 1. Inelastic p-air cross sections in the years 1997 and 2000 (Refs. <sup>14,15,16,17,18,19</sup>).

in the last 3 years, as demonstrated in Fig. 1. The cross section differences between the models have shrunk from 80 mb to today 20 mb in the region at a few PeV. Extrapolations to the highest energies above  $10^{10}$  GeV become much more realistic to make predictions for the Auger experiment.<sup>20</sup>

## 5 Comparison with Collider Data

All models are adjusted to experimental data wherever available. Especially  $p\bar{p}$  collider data should be reproduced with respect to e.g. the increase of average charged particle multiplicity with increasing energy, the spread of the number of emitted charged particles around the mean value according to a negative binomial distribution as shown in Fig. 2a, and the pseudorapidity distribution of emitted charged particles shown together with recent experimental values<sup>22</sup> at  $E_{\text{cm}} = 630$  GeV in Fig. 2b. The more modern models<sup>8,9,10,12</sup> displayed here show good agreement with experimental data. A complete comparison of the older models can be found in Ref.<sup>23</sup>.

For some parameters, the CORSIKA interaction tests revealed differences responsible for deviating properties of EAS simulated with different models. The most frequent hadronic interaction within the development of an EAS cascade is the collision of a charged pion with a  $^{14}\text{N}$  nucleus. Therefore, we compare in Fig. 3a the model predictions of the average charged particle multiplicity produced by this reaction as a function of energy. In general, the higher the multiplicity, the more energy is dissipated into the production of secondaries, which gives rise to a shorter EAS longitudinal distribution. The highest multiplicities are observed for QGSJET. In those events with many secondary particles only a small energy fraction is left for the relic of

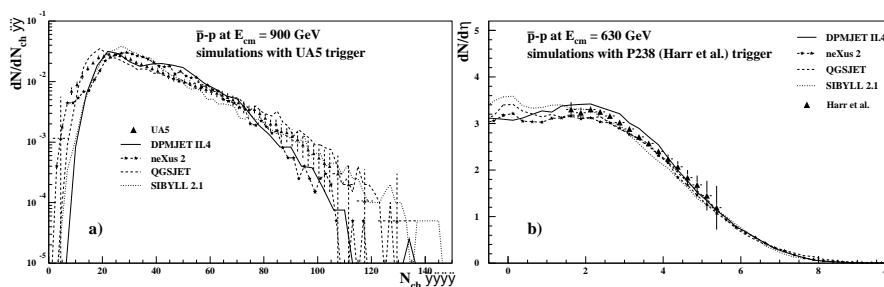


Figure 2. Model adjustments to experimental values<sup>21,22</sup> of  $p\bar{p}$  collisions: Charged particle multiplicities at  $\sqrt{s} = 900$  GeV (a), Charged particle pseudorapidity distributions at  $\sqrt{s} = 630$  GeV (b).

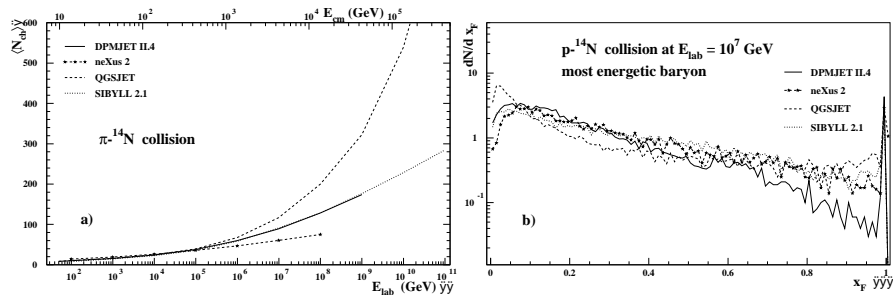


Figure 3. Model predictions for hadron- $^{14}\text{N}$  collisions: Average charged particle multiplicity as a function of energy for  $\pi^-$ - $^{14}\text{N}$  collisions (a), energy fraction (Feynman- $x$ ) distribution of the most energetic baryon from  $p$ - $^{14}\text{N}$  collisions at  $E_{\text{lab}} = 10^7$  GeV (b).

the projectile. This is demonstrated in Fig. 3b, which shows the Feynman- $x$  distribution of the most energetic baryon from  $p$ - $^{14}\text{N}$  collisions. In the range  $0.1 < x_F < 0.4$ , corresponding to a moderate energy transfer to secondary particles, QGSJET exhibits the lowest rate.

Of special interest is the behavior of the Feynman- $x$  distribution of Fig. 3b for values  $x_F \geq 0.85$ . This region is governed by diffractive interactions. In diffractive collisions the projectile loses only a small energy fraction, the largest energy portion is transported deeper into the atmosphere with the projectile remainder. It must be pointed out that describing correctly the diffractive phenomena is of great importance for the hadron rates which are observed at KASCADE level.<sup>24</sup> The large differences between the models reflect the lack of experimental data in the forward region.

## 6 Results of EAS Simulations

Only new or recently revised models<sup>8,9,10,12</sup> are regarded here. A more detailed comparison of the models is given in Ref.<sup>23,25</sup>. All shower properties which can be measured with detectors placed at observation level more or less strongly depend on the ‘age’ of EAS development. As mentioned above, the inelastic hadronic cross sections as well as the ‘inelasticity’ (the fraction of energy carried away by secondary particles) of hadronic interactions are the essential quantities which determine the elongation (slow aging) or shortening (fast aging) of the EAS development.

In Fig. 4a the number of electrons (incl. positrons) is shown as a function of atmospheric depth for vertical showers induced by *protons* or *Fe*-nuclei with energies of  $E_0 = 10^{14}$  and  $10^{15}$  eV. The number (averaged over 500

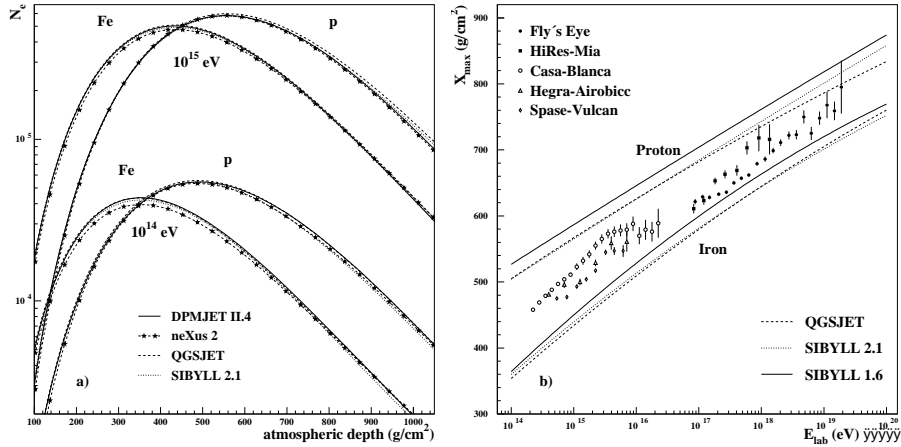


Figure 4. Longitudinal shower development for proton and iron induced vertical showers at primary energies of  $E_0 = 10^{14}$  eV and  $10^{15}$  eV (a). Depth of shower maximum  $X_{\max}$  as a function of energy as predicted by QGSJET and two versions of SIBYLL, together with measurement points of experiments<sup>26,27,28,29,30</sup> (b).

simulated showers each) of electrons at sea level ( $1036 \text{ g/cm}^2$ ) differs between the models by max. 14 % (*proton*) resp. 3 % (*Fe*) at  $10^{15}$  eV, becoming even smaller at lower energies. The differences have shrunk by more than a factor of 3 with respect to a 1997 comparison<sup>25</sup> of the older models.

A quantity measured by several experiments is the depth  $X_{\max}$  (expressed in  $\text{g/cm}^2$ ) of the maximum number of charged particles within the EAS development. The  $X_{\max}$ -value is sensitive to the primary particle type and may be used to determine the (energy dependent) cosmic ray mass composition. Fig. 4b gives a survey of several experiments, which use different techniques (fluorescence<sup>26,27</sup> = filled symbols, Cherenkov<sup>28,29,30</sup> = open symbols) to determine  $X_{\max}$  at various energies, extending over 5 decades.

The model predictions of Fig. 4b are derived from averages over 500 vertical *proton*-induced showers (resp. 200 *Fe*-induced showers) for each of the 13 equidistant reference energies. The uncertainties of the mean  $X_{\max}$  are dominated by shower fluctuations and range from  $5 \text{ g/cm}^2$  at  $10^{14}$  eV to  $3 \text{ g/cm}^2$  at  $10^{20}$  eV for *proton* EAS and amount to about the half for *Fe*. The mean  $X_{\max}$ -values are approximated by quadratic expressions of the form

$$X_{\max} = a + b \cdot \lg E + c \cdot (\lg E)^2 ,$$

which follow the simulated mean values within the error bars.

It must be emphasized that none of the models predicts a linear relation as is often assumed in oversimplified arguments. The elongation rate per energy decade decreases from c. 70 g/cm<sup>2</sup> at 10<sup>14</sup> eV to c. 50 g/cm<sup>2</sup> at 10<sup>20</sup> eV for *proton*-induced showers and shows a similar reduction from c. 80 to c. 60 g/cm<sup>2</sup> for *Fe*-induced showers. Remarkable is the good agreement between QGSJET and SIBYLL 2.1 up to 10<sup>18</sup> eV. At higher energies, SIBYLL predicts a larger  $X_{\max}$ -separation between *proton* and *Fe* showers. The new SIBYLL version 2.1 generally reveals  $X_{\max}$ -values reduced by  $\approx 20$  g/cm<sup>2</sup> relative to the older version 1.6.

## 7 Conclusion

In the last 3 years large progress is attained in EAS simulations. By the reevaluation of inelastic proton-air cross sections, a considerable agreement is achieved now up to the 10<sup>7</sup> GeV range. A clear trend of convergence between different hadronic interaction models is obvious for primary energies up to the 10<sup>6</sup> GeV range. Despite its age, presently QGSJET still shows the best, though not in all respects satisfying agreement with a variety of experimental results.<sup>24,31</sup> The new SIBYLL version<sup>12</sup> and the more modern ideas realized in NEXUS<sup>9</sup> should enable a more consistent and reliable extrapolation especially to the highest energies. The announced<sup>32</sup> version III of DPMJET still has to demonstrate its improved quality.

## Acknowledgments

Many thanks go to the authors of the hadronic interaction models for their help to get their programs running and for their advice in coupling the programs with CORSIKA. I am indebted to R. Engel for making available the new SIBYLL version 2.1. The partial support of this work by the British German Academic Research Collaboration (Grant 313/ARC-lk) is acknowledged.

## References

1. H.O. Klages *et al* (KASCADE Coll.), *Nucl. Phys. B* (Proc. Suppl.) **52B**, 92 (1997).
2. D. Heck *et al*, Report **FZKA 6019** (1998).
3. J. Knapp and D. Heck, Report **KfK 5196B** (1993); updated version see <http://www-ik3.fzk.de/~heck/corsika> (2000).

4. W.R. Nelson, H. Hirayama and D.W.O. Rogers, Report **SLAC 265** (1985).
5. A.A. Lagutin, A.V. Plyasheshnikov and V.V. Uchaikin in *Proc. 16<sup>th</sup> Int. Cosmic Ray Conf.*, Kyoto (Japan), **7**, 18 (1979).
6. H. Fesefeldt, Report **PITHA-85/02**, RWTH Aachen (1985).
7. S.A. Bass *et al*, *Prog. Part. Nucl. Phys.* **41**, 225 (1998); M. Bleicher *et al*, *J. Phys. G: Nucl. Part. Phys.* **25**, 1859 (1999).
8. J. Ranft, *Phys. Rev. D* **51**, 64 (1995); preprint hep-ph/0002137 (2000).
9. H.J. Drescher *et al*, preprint hep-ph/0007198 (2000).
10. N.N. Kalmykov, S.S. Ostapchenko and A.I. Pavlov, *Nucl. Phys. B (Proc. Suppl.)* **52B**, 17 (1997).
11. R.S. Fletcher *et al*, *Phys. Rev. D* **50**, 5710 (1994); J. Engel *et al*, *Phys. Rev. D* **46**, 501 (1992).
12. R. Engel *et al* in *Proc. 26<sup>th</sup> Int. Cosmic Ray Conf.*, Salt Lake City (USA), **1**, 415 (1999); R. Engel, private communication (2000).
13. K. Werner, *Phys. Rep.* **232**, 87 (1993).
14. H.H. Mielke *et al*, *J. Phys. G: Nucl. Part. Phys.* **20**, 637 (1994).
15. G.B. Yodh *et al*, *Phys. Rev. D* **27**, 1183 (1983).
16. R.M. Baltrusaitis *et al*, *Phys. Rev. Lett.* **52**, 1380 (1984).
17. M. Honda *et al*, *Phys. Rev. Lett.* **70**, 525 (1993).
18. M. Aglietta *et al* (EAS-TOP Coll.) in *Proc. 25<sup>th</sup> Int. Cosmic Ray Conf.*, Durban (South Africa), **6**, 37 (1997).
19. M.M. Block *et al*, *Phys. Rev. D* **62**, 077501 (2000).
20. T. Dova (AUGER Coll.) in *Proc. XXX Int. Symp. Multiparticle Dynamics*, eds. T. Csörgö *et al*, (World Scientific, Singapore, 2001).
21. R.E. Ansorge *et al* (UA5 Coll.), *Z. Phys. C* **43**, 357 (1989).
22. R. Harr *et al*, *Phys. Lett. B* **401**, 176 (1997).
23. J. Knapp, D. Heck and G. Schatz, Report **FZKA 5828** (1996).
24. M. Risse *et al* (KASCADE Coll.) in *Proc. 26<sup>th</sup> Int. Cosmic Ray Conf.*, Salt Lake City (USA), **1**, 135 (1999).
25. J. Knapp, *Nucl. Phys. B (Proc. Suppl.)* **75A**, 89 (1999).
26. D. Bird *et al*, *Phys. Rev. Lett.* **71**, 3401 (1993).
27. T. Abu-Zayyad *et al*, preprint astro-ph/0010652 (2000).
28. J.W. Fowler *et al*, preprint astro-ph/0003190 (2000).
29. F. Arqueros *et al* (HEGRA Coll.), *Astron. Astrophys.* **359**, 682 (2000).
30. J.E. Dickinson *et al* in *Proc. 26<sup>th</sup> Int. Cosmic Ray Conf.*, Salt Lake City (USA), **3**, 136 (1999).
31. K.H. Kampert (KASCADE Coll.) in *Proc. XXX Int. Symp. Multipart. Dynamics*, eds. T. Csörgö *et al* (World Scientific, Singapore, 2001).
32. S. Roesler, R. Engel and J. Ranft, preprint hep-ph/0012252 (2000).